Supporting Information

Effects of the number of methoxy groups in the thiophene π-bridge on the Photovoltaic Performance of the A-π-A type Quasi-macromolecular Acceptors

Qinhao Shi,[a] Yijie Nai,[a] Siqing He,[a] Yitong Ji,[b] Weikun Chen,[a] Wei Liu,[a] Wenchao Huang,[b] Jun Yuan*[a] & Yingping Zou*[a]

[a] *College of Chemistry and Chemical Engineering, Central South University, Changsha 410083, China.*

[b] *School of Materials Science and Engineering, Wuhan University of Technology, Wuhan 430070, China.*

* Corresponding E-mail: junyuan@csu.edu.cn (Yuan J); yingpingzou@csu.edu.cn (Zou Y)

1. Experimental Section

Materials and Synthesis

2,5-Bis(trimethylstannyl)thiophene was purchased from Aladdin, 3-methoxy-2,5-bis(trimethylstannane)thiophene and 3,4-dimethoxy-2,5-bis(trimethylstannane)thiophene were purchased from SunaTech Inc, 2-(5,6-difluoro-3-oxo-2,3-dihydro-1H-inden-1-ylidene)malononitrile was purchased from Adamas. 2-(5-Bromo-3-oxo-2,3-dihydro-1H-inden-1-ylidene)malononitrile was self-made based on a published work[1] and used to preparing BTP-BO-2F-Br. Other reagents and chemicals were purchased from Energy Chemical. The detailed synthetic procedures of QM-T, OM-OT, QM-DOT are shown as following.

Synthesis of BTP-BO-2F-Br

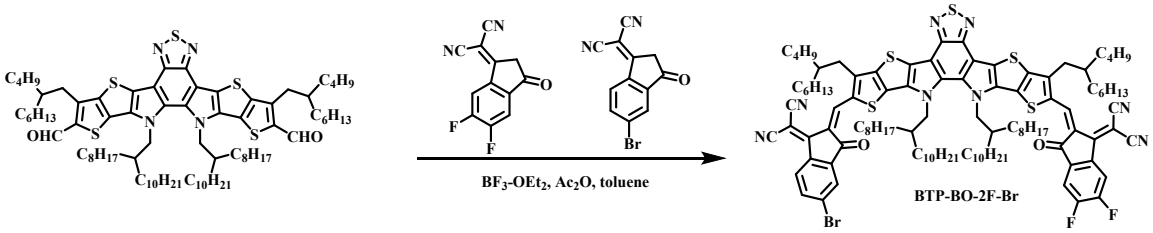

Fig. S1 Synthetic route of BTP-BO-2F-Br.

The compound BTP-BO-CHO (1.05 g, 0.754 mmol), IC-2F (0.191 g, 0.830 mmol), and IC-Br (0.227 g, 0.80 mmol) were added to a 250 mL single-necked round-bottomed flask, dissolved in 130 mL of toluene stirring, then 1.0 mL of acetic anhydride and 1.0 mL of boron fluoride ethyl ether were added. The reaction was carried out at room temperature for about 1 h until no fluorescent spots were observed by TLC. After the reaction was completed, the solution was poured into methanol for precipitation. The filtered solid was dissolved in dichloromethane, and then purified by column chromatography with petroleum ether/dichloromethane (2:1, *v*/*v*) as an eluent. Finally, 0.687 g (yield 49 %) of blue black solid BTP-BO-2F-Br was obtained. ^{1}H NMR (500 MHz, $CDCl_3$) δ 9.17 (d, J = 6.8 Hz, 2H), 8.58 (dd, J = 9.2, 5.2 Hz, 2H), 8.03 (d, J = 1.9 Hz, 1H), 7.87 (dd, J = 8.4, 2.0

Hz, 1H), 7.70 (t, *J* = 7.5 Hz, 1H), 4.77 (d, *J* = 7.8 Hz, 4H), 3.19 (dd, *J* = 7.7, 3.4 Hz, 4H), 2.16 - 2.06 (m, 4H), 1.46 - 1.23 (m, 38H), 1.18 - 0.94 (m, 55H), 0.89 - 0.78 (m, 27H).

Synthesis of QM-T

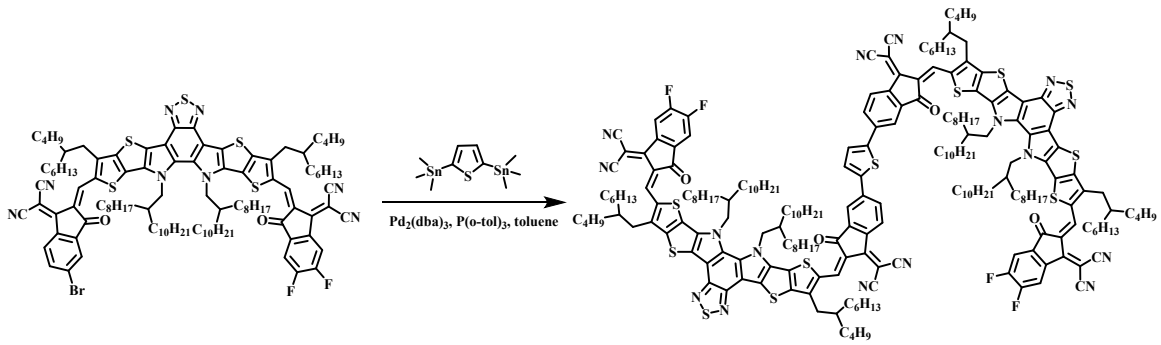

Fig. S2 Synthetic route of QM-T.

The compound BTP-BO-2F-Br (104.0 mg, 0.0559 mmol), 2,5-bis(trimethylstannyl) thiophene (10.9 mg, 0.0266 mmol), $Pd_2(dba)_3$ (3.7 mg, 0.00399 mmol) and $P(o\text{-}tol)_3$ (14.6 mg, 0.0479 mmol) were dissolved in 20 mL anhydrous and deoxidized toluene, then the mixture was stirred at 110℃ for 3 h under argon. The reaction process was monitored by TLC. After the reaction was completed, the solution was poured into methanol for precipitation. The filtered solid was dissolved in dichloromethane, and then purified by column chromatography with petroleum ether/dichloromethane (1:1, v/v) as an eluent. Finally, 59 mg (yield 61%) of black solid QM-T was obtained. ^{1}H NMR (500 MHz, $CDCl_3$) δ 9.15 (s, 4H), 8.78 (d, *J* = 8.3 Hz, 2H), 8.58 (dd, *J* = 9.9, 6.4 Hz, 2H), 8.11 (s, 2H), 7.99 (d, *J* = 8.6 Hz, 2H), 7.70 - 7.62 (m, 4H), 4.89 - 4.72 (m, 8H), 3.16 (dd, *J* = 17.2, 7.3 Hz, 8H), 2.19 - 2.06 (m, 8H), 1.50 - 1.10 (m, 131H), 1.08 - 0.94 (m, 74H), 0.82 (m, 62H). ^{13}C NMR (125 MHz, $CDCl_3$) δ 187.75, 185.90, 159.93, 158.95, 155.33, 153.51, 153.38, 153.32, 153.20, 153.03, 147.58, 147.54, 145.30, 145.27, 143.88, 139.02, 138.94, 137.91, 137.86, 137.52, 136.60, 135.95, 135.58, 135.45, 134.49, 134.38, 134.34, 134.11, 133.86, 131.21, 131.01, 130.47, 127.18, 126.04, 120.90, 119.91, 118.92, 115.81, 115.26, 115.16, 115.00, 114.83, 114.61, 113.70, 113.41, 112.40, 112.25, 77.28, 77.03, 76.77, 68.65, 67.63, 55.90, 40.04, 39.87, 39.24, 39.17, 34.70, 34.44, 33.58, 33.32, 33.26, 31.95, 31.92, 31.87, 31.86, 30.64, 29.85, 29.82, 29.77, 29.74, 29.69, 29.67, 29.65, 29.62, 29.58, 29.48, 29.43,

29.39, 29.37, 29.27, 29.23, 28.85, 28.83, 26.59, 25.72, 23.02, 23.00, 22.70, 22.67, 14.12, 14.11, 14.08, 14.05. HRMS (MALDI-TOF) m/z: [M^+], calcd for $C_{220}H_{280}F_4N_{16}O_4S_{11}$ 3639.9130, found 3639.4260.

Synthesis of QM-OT

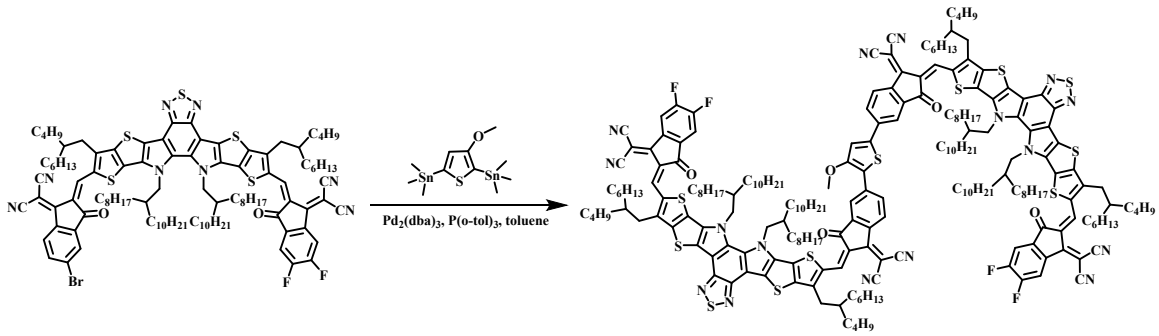

Fig. S3 Synthetic route of QM-OT.

The compound BTP-BO-2F-Br (80.0 mg, 0.0430 mmol), 3-methoxy-2,5-bis (trimethylstannane)thiophene (9.0 mg, 0.0205 mmol), $Pd_2(dba)_3$ (2.8 mg, 0.00307 mmol) and P(o-tol)$_3$ (11.2 mg, 0.0369 mmol) were dissolved in 20 mL anhydrous and deoxidized toluene, then the mixture was stirred at 110℃ for 3 h under argon. The reaction process was monitored by TLC. After the reaction was completed, the solution was poured into methanol for precipitation. The filtered solid was dissolved in dichloromethane, and then purified by column chromatography with petroleum ether/dichloromethane (1:1, *v*/*v*) as an eluent. Finally, 43 mg (yield 57%) of black solid QM-OT was obtained. ^{1}H NMR (500 MHz, $CDCl_3$) δ 9.11 (d, *J* = 16.8 Hz, 4H), 8.74 (dd, *J* = 12.2, 8.2 Hz, 2H), 8.62 - 8.51 (m, 2H), 8.42 - 8.24 (m, 1H), 8.09 (s, 2H), 7.95 (d, *J* = 8.4 Hz, 1H), 7.66 (td, *J* = 7.5, 2.6 Hz, 2H), 7.45 (s, 1H), 4.81 (d, J = 7.8 Hz, 8H), 4.19 (s, 3H), 3.15 (t, *J* = 9.8 Hz, 8H), 2.10 (dd, *J* = 26.3, 17.8 Hz, 8H), 1.50 - 1.12 (m, 100H), 1.03 (s, 70H), 0.90 - 0.74 (m, 52H). ^{13}C NMR (125 MHz, $CDCl_3$) δ 187.73, 185.87, 158.93, 157.69, 155.30, 153.49, 153.19, 152.49, 147.56, 145.31, 145.26, 145.15, 140.06, 138.90, 138.10, 138.00, 137.79, 137.53, 137.36, 136.53, 136.02, 135.94, 135.54, 134.97, 134.46, 134.31, 134.12, 134.08, 133.84, 131.71, 130.92, 130.55, 129.99, 126.02, 125.65, 120.72, 119.90, 115.72, 115.44, 115.21, 114.99, 114.85, 114.63, 113.78, 113.42, 113.18, 112.24, 77.28, 77.03, 76.77, 68.63, 68.51,

66.93, 66.81, 59.08, 55.92, 40.02, 39.89, 39.76, 39.24, 34.67, 33.57, 33.32, 33.25, 31.95, 31.93, 31.87, 31.83, 30.69, 30.54, 29.87, 29.73, 29.70, 29.67, 29.64, 29.63, 29.57, 29.50, 29.42, 29.40, 29.38, 29.34, 29.30, 29.28, 29.21, 28.85, 26.60, 25.66, 23.02, 22.70, 22.68, 22.65, 14.12, 14.11, 14.05. HRMS (MALDI-TOF) m/z: [M^+], calcd for $C_{221}H_{282}F_4N_{16}O_5S_{11}$ 3669.9235, found 3669.7090.

Synthesis of QM-DOT

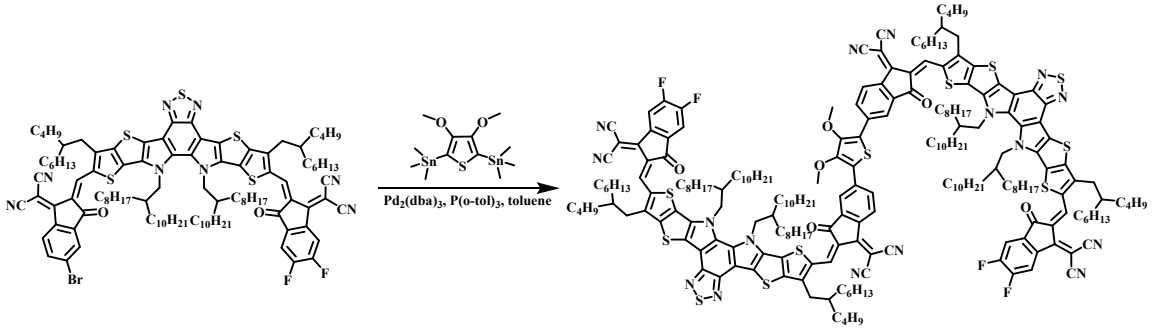

Fig. S4 Synthetic route of QM-DOT.

The compound BTP-BO-2F-Br (67.0 mg, 0.0358 mmol), 3,4-dimethoxy-2,5-bis (trimethylstannane)thiophene (8.0 mg, 0.0170 mmol), $Pd_2(dba)_3$ (2.4 mg, 0.00255 mmol) and $P(o\text{-}tol)_3$ (9.3 mg, 0.0306 mmol) were dissolved in 20 mL anhydrous and deoxidized toluene, then the mixture was stirred at 110℃ for 3 h under argon. The reaction process was monitored by TLC. After the reaction was completed, the solution was poured into methanol for precipitation. The filtered solid was dissolved in dichloromethane, and then purified by column chromatography with petroleum ether/dichloromethane (1:1, *v*/*v*) as an eluent. Finally, 37 mg (yield 59%) of black solid QM-DOT was obtained. ^{1}H NMR (500 MHz, $CDCl_3$) δ 9.17 (d, *J* = 18.7 Hz, 4H), 8.78 (d, *J* = 8.4 Hz, 2H), 8.58 (dd, *J* = 9.9, 6.4 Hz, 2H), 8.40 (s, 2H), 8.14 (d, *J* = 8.6 Hz, 2H), 7.64 (t, *J* = 7.5 Hz, 2H), 4.79 (t, *J* = 6.0 Hz, 8H), 4.07 (s, 6H), 3.19 (dd, *J* = 12.2, 7.5 Hz, 8H), 2.12 (d, *J* = 20.3 Hz, 8H), 1.51 - 1.22 (m, 71H), 1.20 - 0.94 (m, 116H), 0.91 - 0.74 (m, 58H). ^{13}C NMR (125 MHz, $CDCl_3$) δ 188.01, 185.89, 160.19, 158.96, 155.35, 153.50, 153.37, 153.29, 153.18, 152.74, 150.17, 147.54, 147.51, 145.26, 138.60, 138.29, 137.97, 137.71, 137.47, 136.58, 135.91, 135.58, 135.33, 135.15, 134.46, 134.33, 134.09, 133.77, 131.94, 130.96, 130.31, 125.80, 124.37, 121.27, 120.40, 119.88, 115.73, 115.24, 115.16, 115.01, 114.84, 114.62, 113.76, 113.32,

112.37, 112.21, 77.28, 77.03, 76.77, 68.62, 67.55, 60.59, 55.88, 55.77, 40.03, 39.95, 39.15, 34.65, 33.58, 33.31, 31.93, 31.88, 31.86, 31.82, 30.61, 30.55, 29.81, 29.73, 29.71, 29.67, 29.62, 29.58, 29.56, 29.46, 29.39, 29.37, 29.32, 29.24, 29.20, 28.86, 26.60, 25.61, 23.03, 23.01, 22.69, 22.66, 22.64, 14.11, 14.08. HRMS (MALDI-TOF) m/z: [M^+], calcd for $C_{222}H_{284}F_4N_{16}O_6S_{11}$ 3699.9341, found 3699.5041.

2. Instruments and Measurements

^{1}H NMR and ^{13}C NMR spectra were recorded using a Bruker AV-500 spectrometer in a deuterated chloroform solution at 298 K, unless specified otherwise. Chemical shifts are reported as δ values (ppm) with tetramethylsilane (TMS) as the internal reference. The molecular mass (MS) was confirmed using an Autoflex III matrix-assisted laser desorption ionization mass spectrometer (MALDI-TOF-MS). Thermogravimetric analysis (TGA) was conducted on a TGA8000-FTIR-GCMS-ATD with a heating rate of 10°C/min under helium. Different scanning calorimetry (DSC) was conducted on a STA8000 at a scan rate of 10°C/min under helium. UV-Vis absorption spectra were recorded on the SHIMADZU UV-2600 spectrophotometer. Films were coated on the quartz plates and the Chloroform solution of QM acceptors was contained in a 0.1 mm slit-width cuvette at room temperature. The cyclic voltammetry (CV) results were obtained with a computer-controlled CHI660E electrochemical workstation. A Pt plate working electrode, a Pt wire counter electrode, and an Ag/AgCl reference electrode were referred to as the three electrodes. The solutions of QM acceptors were dropped onto the working electrode to form thin films, and ferrocene/ferrocenium (Fc/Fc^+) redox couple was used as an internal standard. The HOMO and LUMO energy levels of the PM6 and QM acceptors were calculated from the onset oxidation potential (E_{ox}) and the reduction potential (E_{red}). Atomic force microscopy (AFM, Agilent Technologies, 5500 AFM/SPM System, USA) were used to get the morphologies of the PM6:acceptor blend films in contacting mode with a 2 μm scanner. Transmission electron microscopy (TEM) measurements were performed in a JEM-F200. Samples for the TEM measurements were prepared as following: The active layer films were spin-cast on ITO/PEDOT:PSS substrates, and the substrates with active layers were submerged in deionized water to make the active layers float onto the air-water interface. Then, the floated films were picked upon unsupported

200 mesh copper grids for the TEM measurements. Grazing-incidence wide-angle X-ray scattering (GIWAXS) measurements were accomplished with a Xeuss 3.0 SAXS/WAXS laboratory beamline using a Cu X-ray source (8.05 keV, 1.54 Å) and a Pilatus 100K detector. The incident angle was 0.18° and the detector distance was 75 mm. GIWAXS samples were prepared on silicon substrate by spin coating.

3. Device Fabrication

Organic solar cell devices with ITO/2PACz/Active Layer/PNDIT-F3N/Ag structures were fabricated according to the following processes. Patterned ITO glass substrates were sequentially cleaned by ultrasonicating in acetone, detergent, deionized water, and isopropyl alcohol for 15 min each and then were dried under a dry oven. The cleaned substrates were treated in an ultraviolet-ozone chamber for 15 min before they were transferred into the glove box. The hole transporting layer 2PACz was spin-coated onto the ITO substrates, followed by thermal annealing at 100°C for 10 min. The mixture of PM6:QM-T, PM6:QM-OT, PM6:QM-DOT was dissolved in chloroform (D/A weight ratio of 1:1.2, 15.4 mg mL^{-1}, with 0.6% 1-CN) and stirred for 1 hour. The blend solution was spun onto the 2PACz layer at 3800 rpm for 30s and then thermally annealed at 100℃ for 10 min. After cooling to room temperature, a ~5 nm thick of PNDIT-F3N (1 mg mL^{-1}, 3000 rpm) was spin-coated on the top of the active layer. Finally, under the vacuum condition of 1.5×10^{-4} pa, the Ag was steamed and deposited on the PNDIT-F3N buffer layer through the mask plate as the top electrode, the thickness of Ag is about 120 nm.

4. Device Characterization

Current density-voltage (*J-V*) curves

Current density-voltage (*J-V*) curves of the devices were performed by a Keithley 2400 source meter in a glove box with a nitrogen atmosphere. The simulated sunlight was calibrated by an AM 1.5G solar simulator (Enlitech, SS-F5-3A, Taiwan), which was measured with a calibrated Si diode from National Renewable Energy Laboratory. EQE spectral measurements were performed on a commercial EQE measurement system (Enlitech, QE-R, Taiwan).

Space-charge-limited current (SCLC) measurements

Electron mobility and hole mobility measurements. The electron mobility device adopted the ITO/ZnO/Active Layer/PNDIT-F3N/Al structure, and the hole mobility device adopted the ITO/PEDOT:PSS/Active Layer/MoO_3/Ag structure. The electron and hole mobilities were calculated according to the space charge limited current (SCLC) method by the equation: $J = 9\,\varepsilon_r \varepsilon_0 \mu V^2/8L^3$, where J is the current density, μ is the electron or hole mobility, V is the internal voltage in the device, ε_r is the relative dielectric constant of active layer material, ε_r=3, ε_0 is the permittivity of empty space, ε_0=8.85 *10^{-12} F/m, and L is the thickness of the active layer.

J_{SC} and V_{OC} on the light intensity (P_{light}) dependence

The correlation between J_{SC} and light intensity (P_{light}) can be expressed as $J_{SC} \propto P_{light}^{\alpha}$, where α presents the degree of bimolecular recombination. There will be less bimolecular recombination in devices when α is closer to 1. The correlation between V_{OC} and P_{light} can be expressed by $V_{OC} \propto$ nkT/qln(P_{light}). Generally, with a slope close to kT/q (where k is the Boltzmann constant, T is the temperature in Kelvin, and q is the elementary charge), trap-assisted recombination should be negligible.

5. ^{1}H NMR, ^{13}C NMR, and High-Resolution Mass (MOLDI-TOF) Spectra

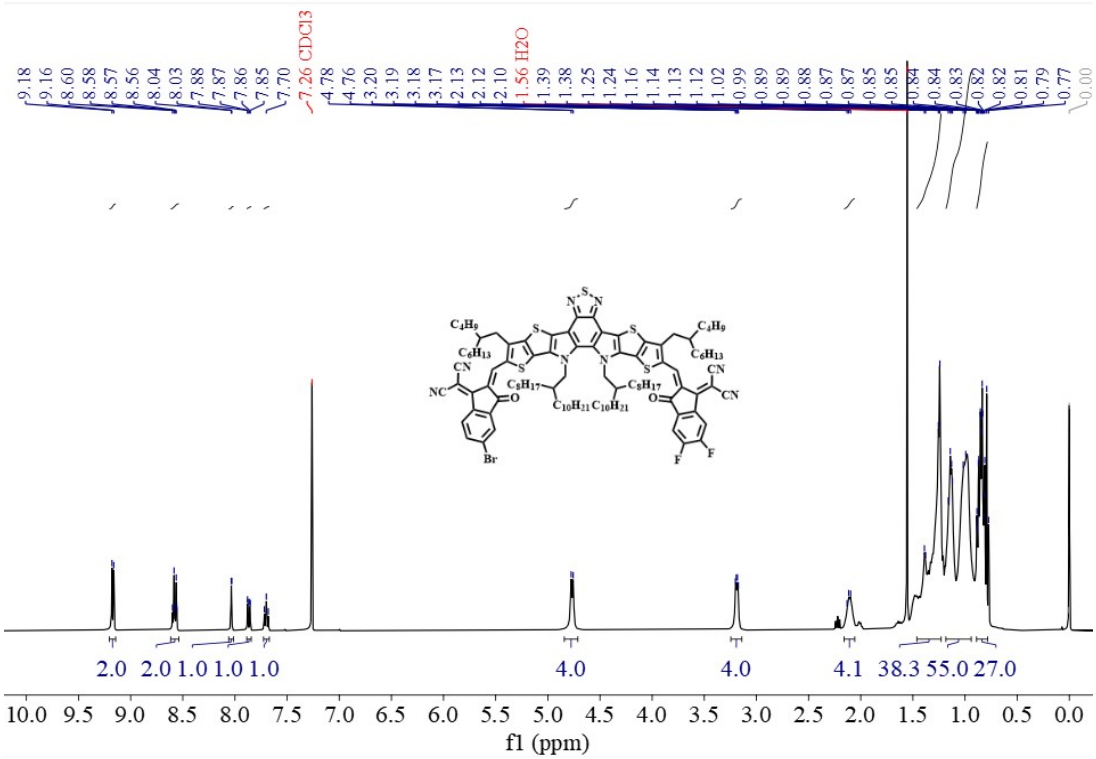

Fig. S5 ^{1}H NMR spectrum of BTP-BO-2F-Br in $CDCl_3$.

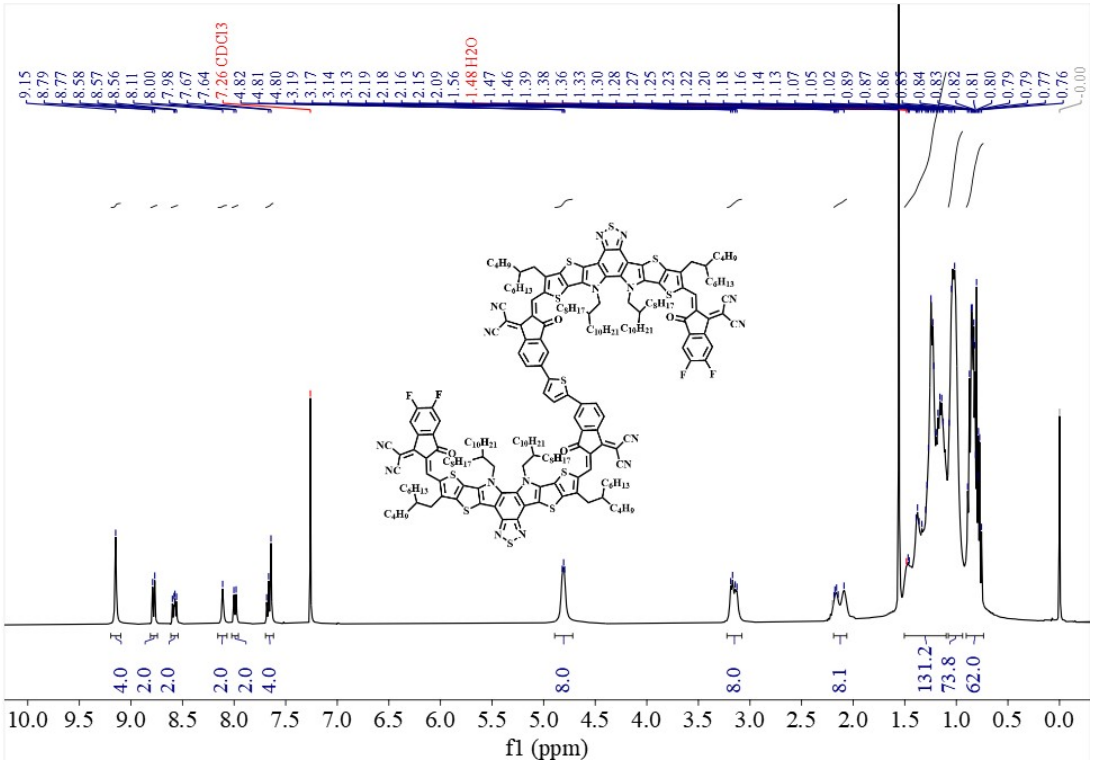

Fig. S6 ^{1}H NMR spectrum of QM-T in $CDCl_3$.

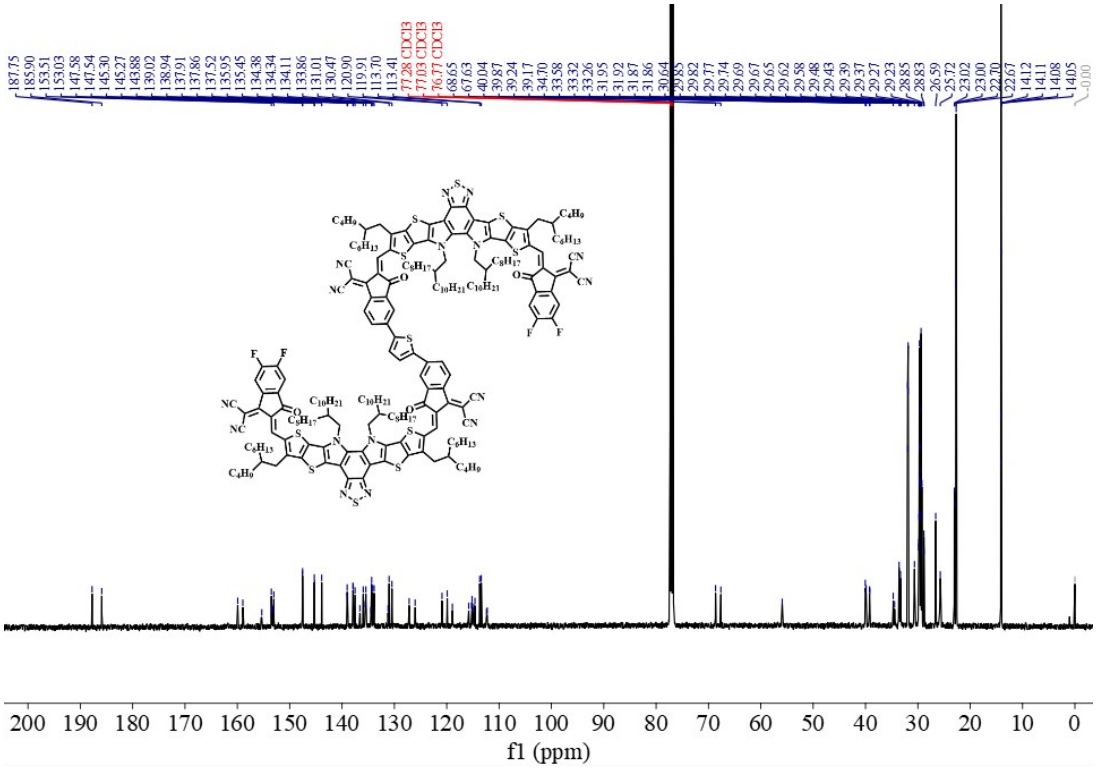

Fig. S7 ^{13}C NMR spectrum of QM-T in $CDCl_3$.

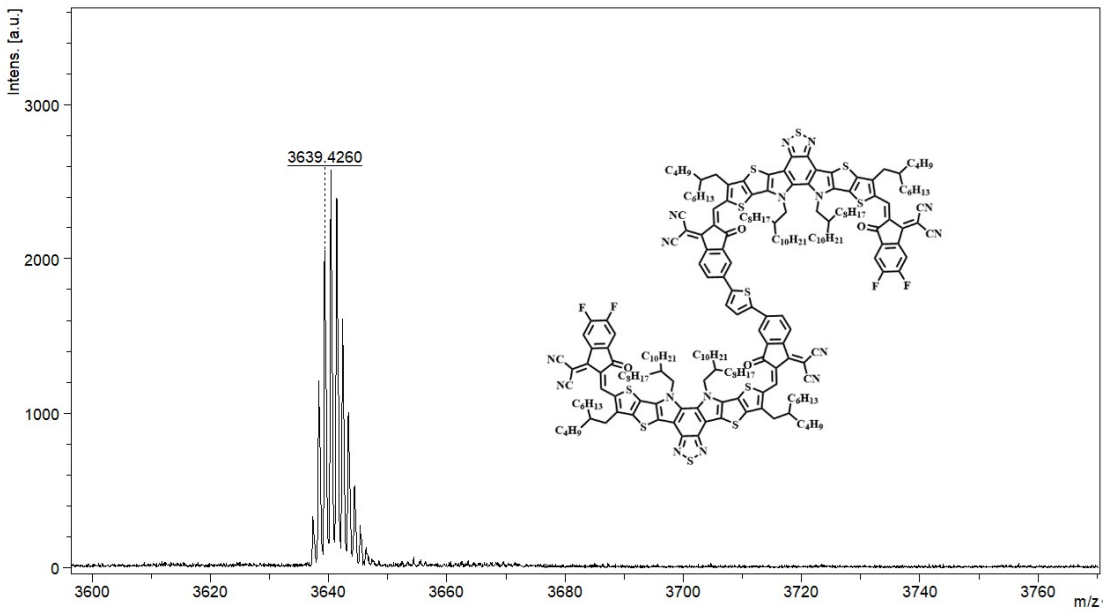

Fig. S8 The high-resolution mass spectrum (MALDI-TOF) of QM-T.

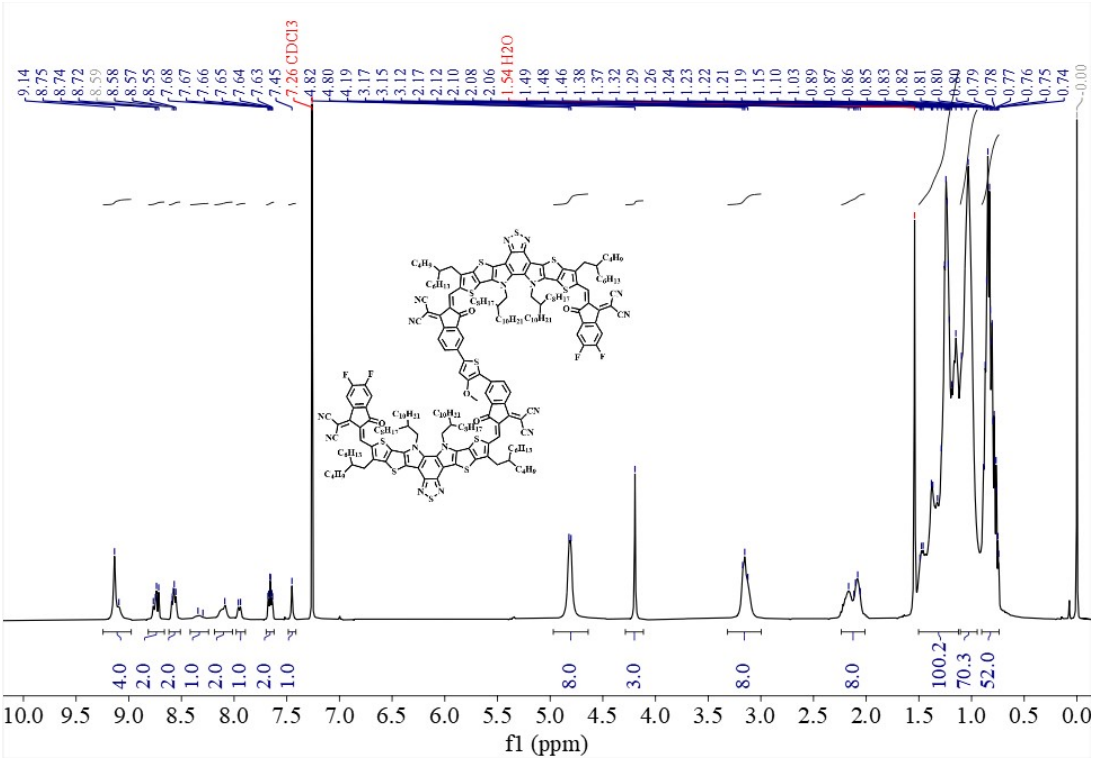

Fig. S9 ^{1}H NMR spectrum of QM-OT in $CDCl_3$.

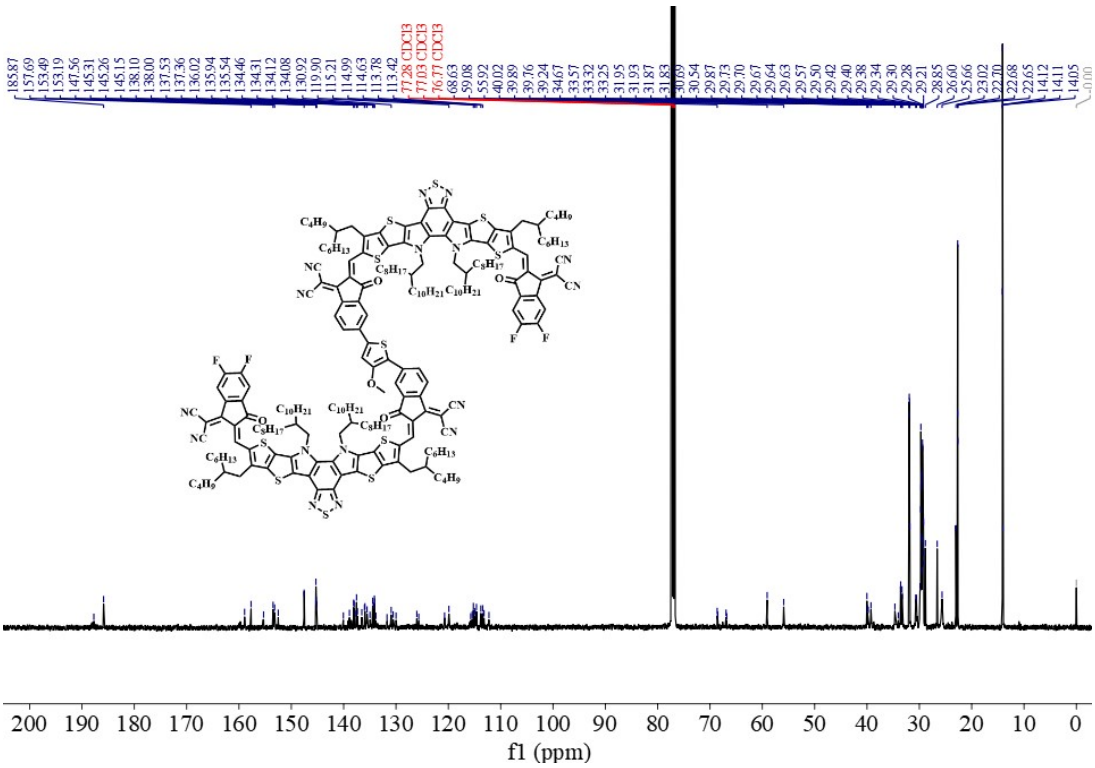

Fig. S10 ^{13}C NMR spectrum of QM-OT in $CDCl_3$.

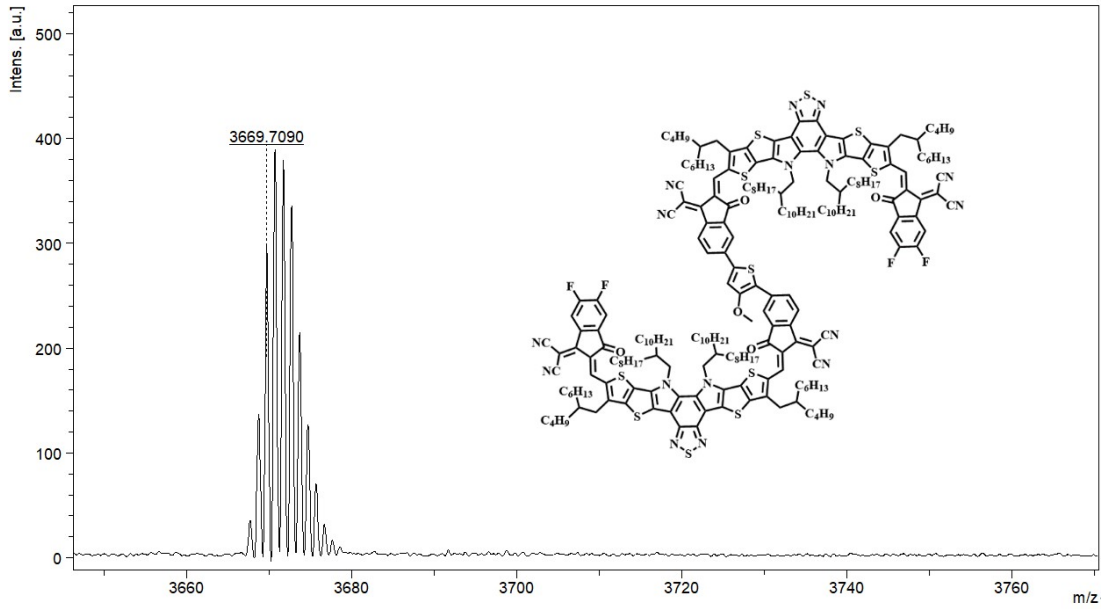

Fig. S11 The high-resolution mass spectrum (MALDI-TOF) of QM-OT.

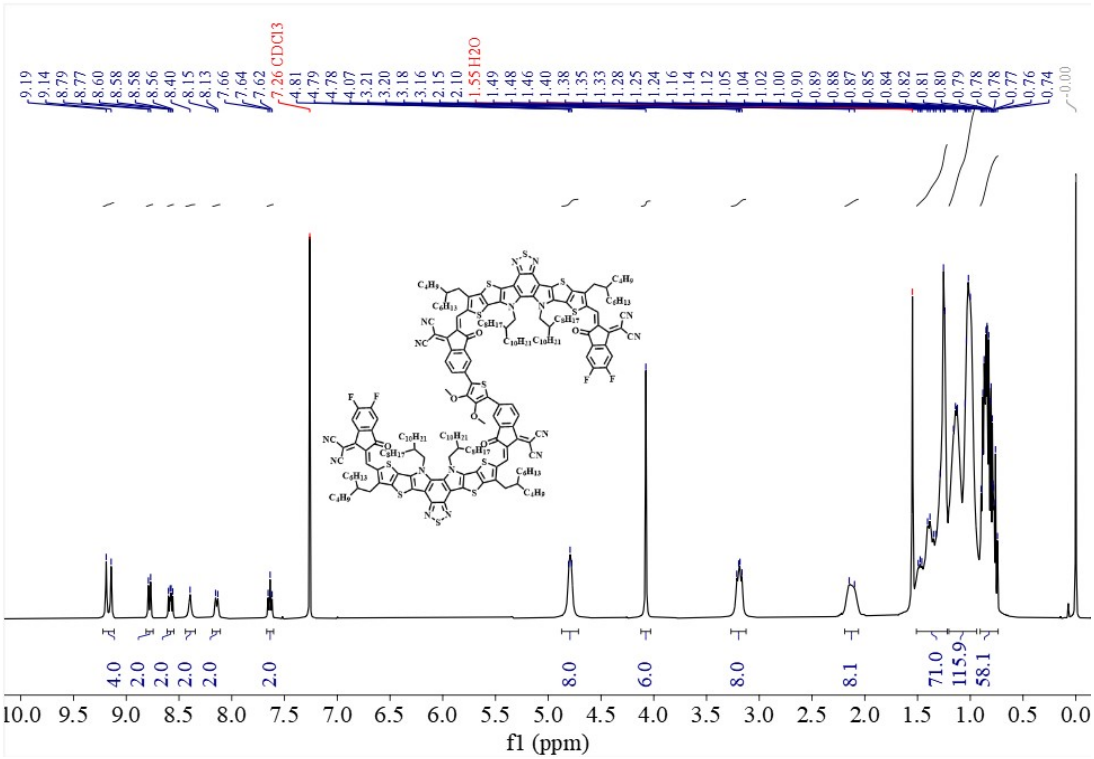

Fig. S12 ^{1}H NMR spectrum of QM-DOT in $CDCl_3$.

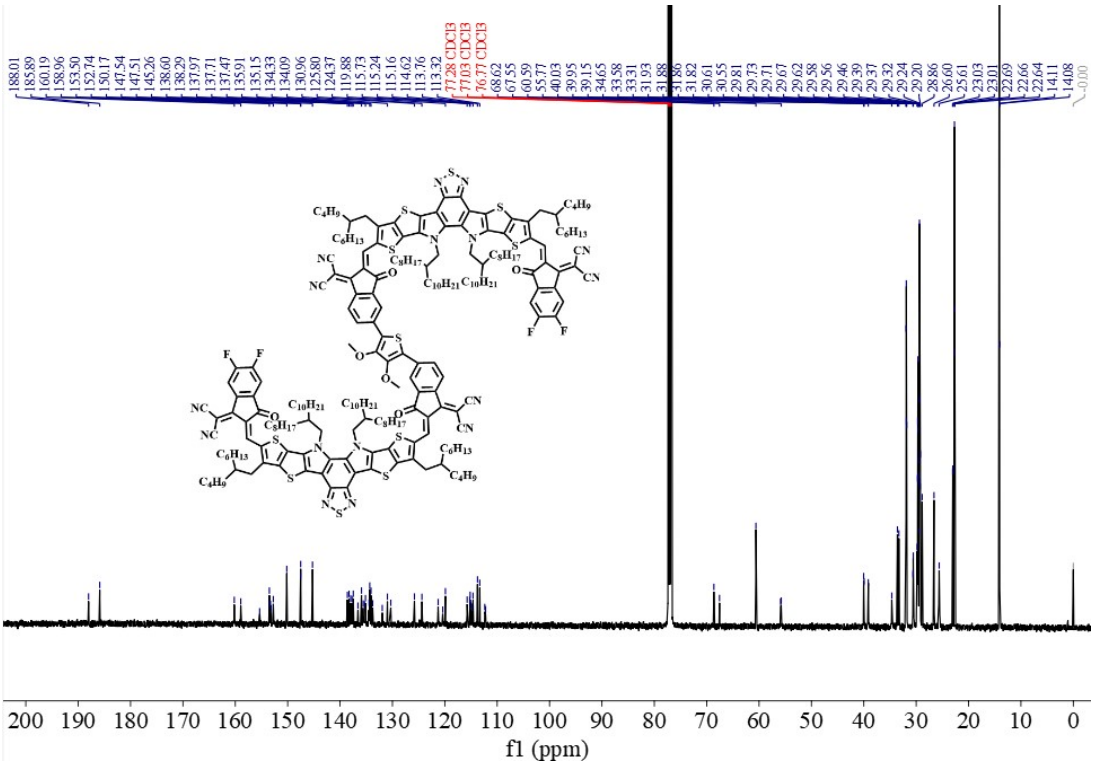

Fig. S13 ^{13}C NMR spectrum of QM-DOT in $CDCl_3$.

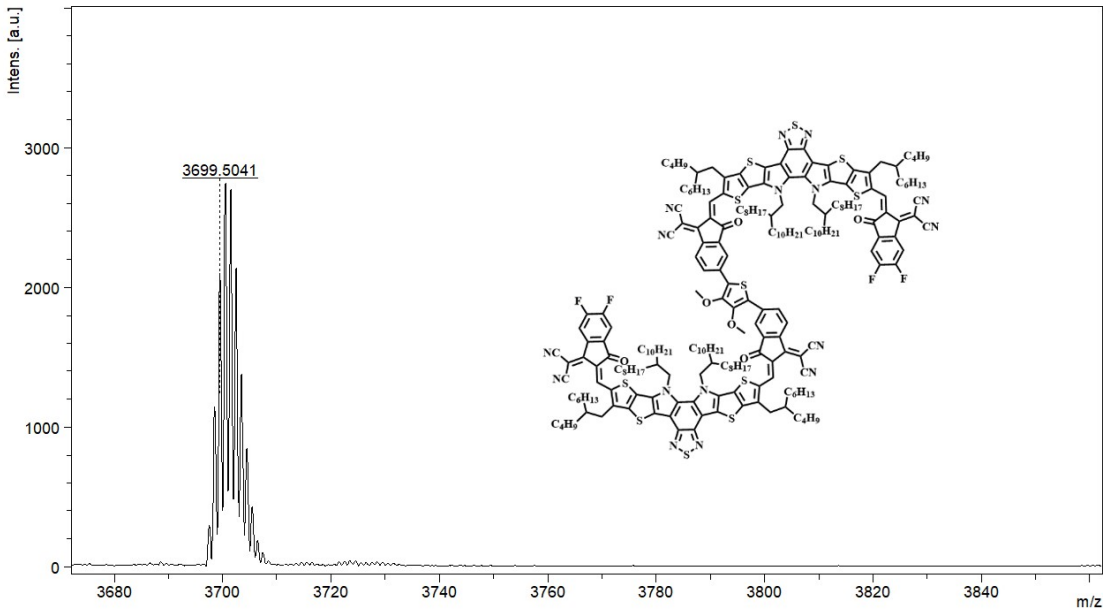

Fig. S14 The high-resolution mass spectrum (MALDI-TOF) of QM-DOT.

6. Additional Figures and Tables

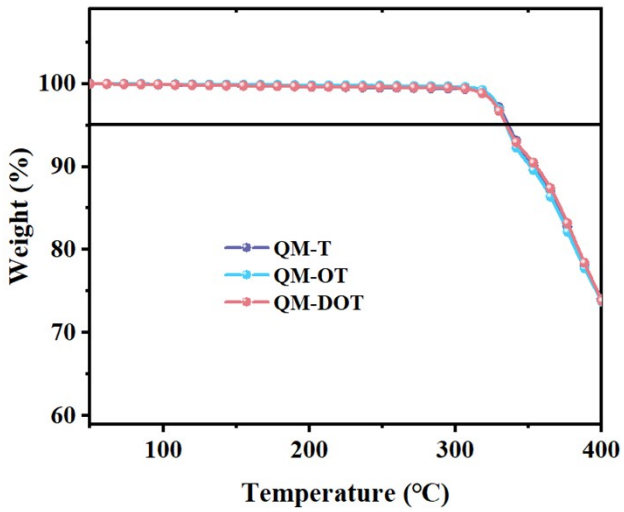

Fig. S15 Thermogravimetric analysis curves of QM-T, QM-OT, QM-DOT with a heating rate of 10℃/min.

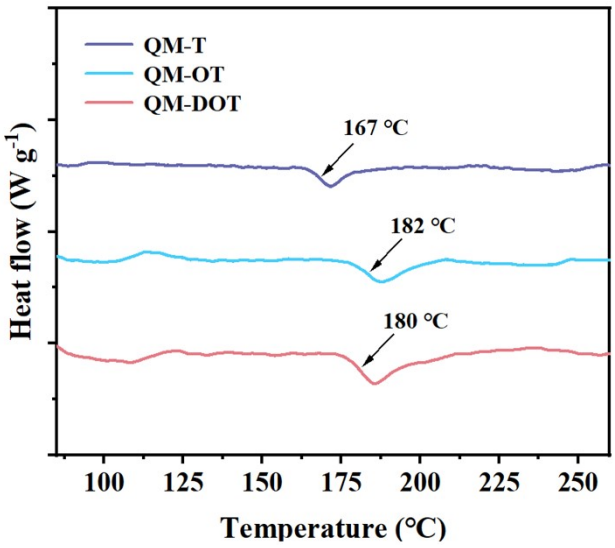

Fig. S16 DSC curves of QM-T, QM-OT, QM-DOT at a scan rate of 10℃/min.

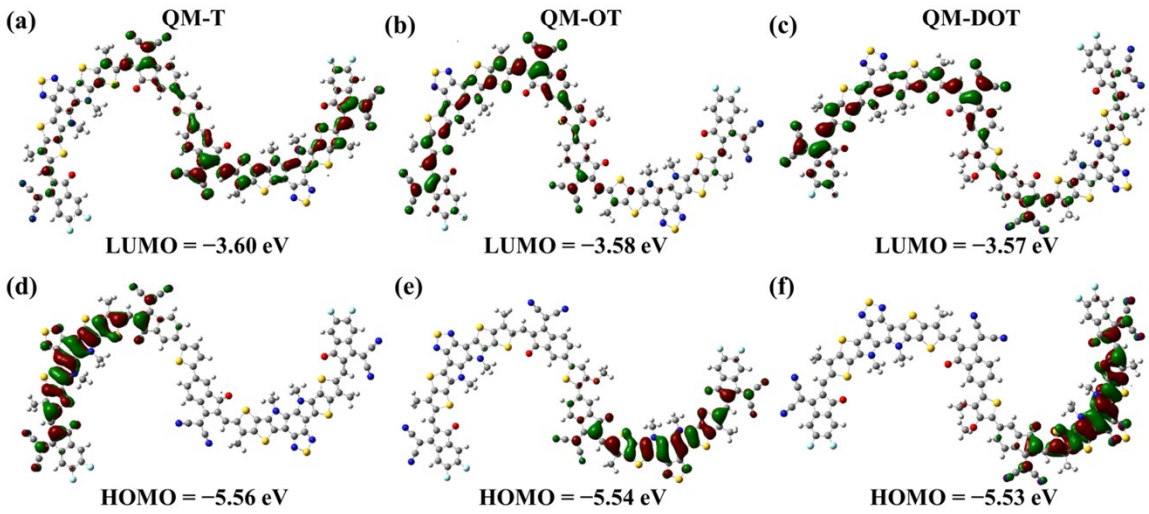

Fig. S17 (a-f) DFT calculated LUMO/HOMO energy levels of QM-T, QM-OT and QM-DOT, respectively.

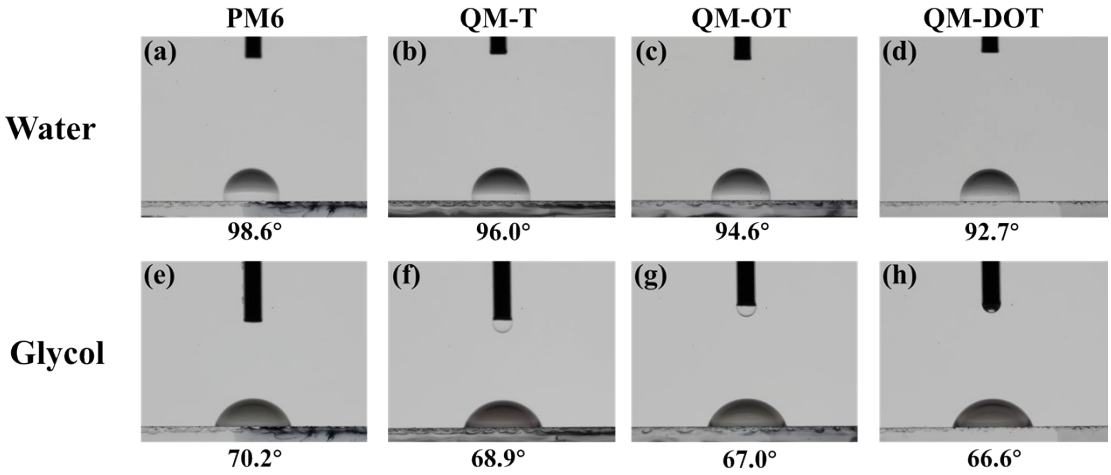

Fig. S18 Contact angle images of water and ethylene glycol droplets on the neat films of PM6, QM-T, QM-OT and QM-DOT.

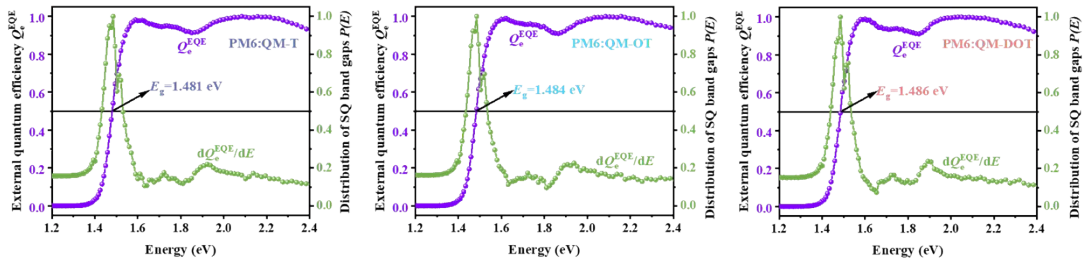

Fig. S19 The extracted E_g from the derivative of the EQE edge.

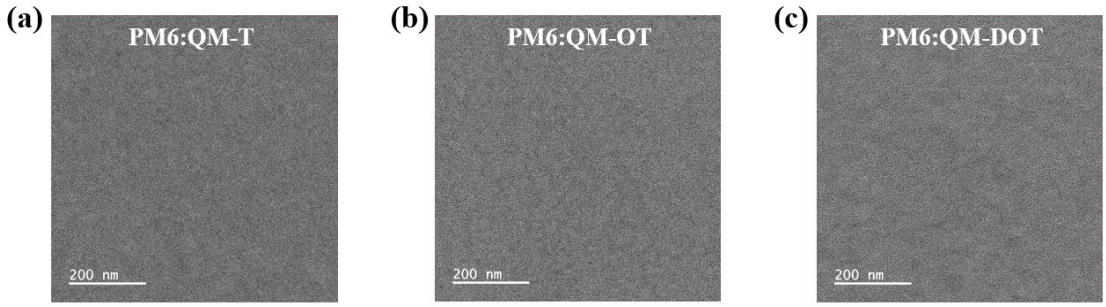

Fig. S20 TEM images of (a) PM6:QM-T, (b) PM6:QM-OT and (c) PM6:QM-DOT blended films.

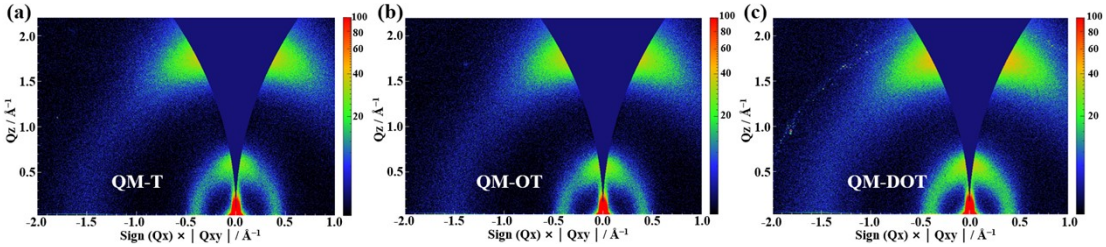

Fig. S21 2D-GIWAXS patterns of (a) QM-T, (b) QM-OT, (c) QM-DOT neat films.

Table S1 Contact angle and statistical data of surface tension and interaction parameter

Material	Water	Clycol	γ (mN m^{-1})	χ
PM6	98.6°	70.2°	32.86	/
QM-T	96.0°	68.9°	30.51	0.044K
QM-OT	94.6°	67.0°	31.49	0.015K
QM-DOT	92.7°	66.6°	29.16	0.110K

Table S2 Energy loss of the devices in this work

Device	E_g (eV)	V_{OC} (V)	E_{loss} (eV)
PM6:QM-T	1.481	0.942	0.539
QM6:QM-OT	1.484	0.956	0.528
PM6:QM-DOT	1.486	0.951	0.535

$E_{loss} = E_g - q\ V_{OC}$

References:

1 Z. Luo, T. Liu, R. Ma, Y. Xiao, L. Zhan, G. Zhang, H. Sun, F. Ni, G. Chai and J. Wang, *Adv. Mater.*, 2020, **32**, 2005942.